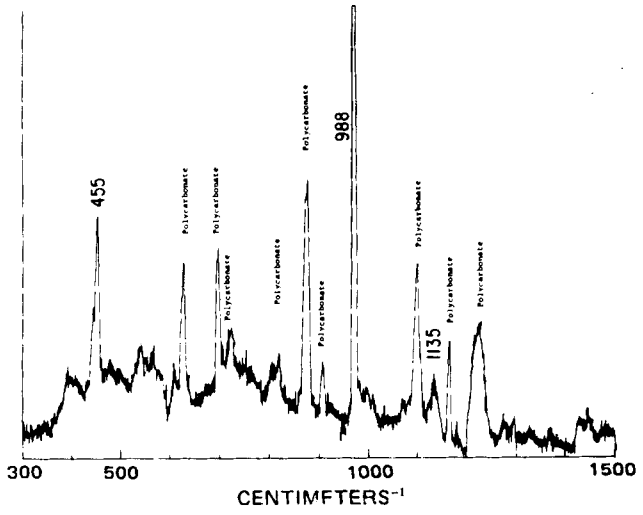

Figure 3—*Raman spectrum of barium sulfate crystal isolated from a parenteral product on a 0.45-μm polycarbonate filter (Nuclepore Corp., Pleasanton, Calif.). Peaks due to the crystal appear at 455, 988, and 1135 cm^{-1}.*

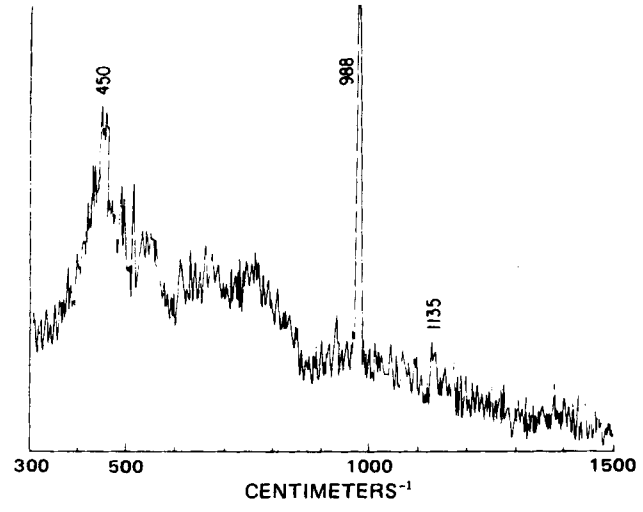

Figure 4—*Raman spectrum of reference barium sulfate crystals on a glass slide showing peaks at 450, 988, and 1135 cm^{-1}.*

In a preliminary experiment, we were able to generate barium sulfate crystals in 10-ml ampuls containing particulate-free solutions of either 0.2% sodium sulfate or 0.2% sodium bisulfite. These ampuls were autoclaved for 2 hr and stored at room temperature for 30 days. Ampuls containing particulate-free water treated identically did not produce any crystals.

Barium sulfate is so insoluble that it can be tolerated orally since it is the barium ion that is highly toxic. However, crystals injected intravenously will lodge in various tissues, depending on their size, and can cause irritation. Therefore, it is important to define the conditions under which barium sulfate crystals form in parenteral products and to devise a means for preventing their formation, such as siliconizing the glass surface or adding either a complexing agent (*i.e.*, ethylenediaminetetraacetic acid) or a nucleation inhibitor (*i.e.*, polyvinylpyrrolidone).

(1) E. J. Bruning, *Virchows Arch.*, **327**, 460 (1955).
(2) S. Sarrut and C. Nezelof, *Presse Med.*, **68**, 375 (1960).
(3) J. M. Garvan and B. W. Gunner, *Med. J. Aust.*, **2**, 140 (1963).
(4) *Ibid.*, **2**, 1 (1964).
(5) P. P. DeLuca, R. Rapp, B. Bivins, H. McKean, and W. Griffen, *Am. J. Hosp. Pharm.*, **32**, 1001 (1975).
(6) H. G. Schroeder and P. P. DeLuca, *ibid.*, **33**, 543 (1976).
(7) S. Rusmin, R. Rapp, B. Bivins, and P. P. DeLuca, *Bull. Parent. Drug Assoc.*, **31**, 1 (1977).
(8) W. C. McCrone and J. G. Delly, "The Particle Atlas, Edition II," vol. III, Ann Arbor Science Publishers, Ann Arbor, Mich., 1973, p. 747.
(9) *Ibid.*, pp. 119–129.
(10) "X-Ray Powder Data File No. 5-0488," ASTM Special Technical Publication 48-J, American Society for Testing and Materials, Philadelphia, Pa., 1960, p. 622.
(11) S. V. Sanga, *J. Parent. Drug Assoc.*, **33**, 61 (1979).

Sam Boddapati
L. David Butler
Sophann Im
Patrick P. DeLuca ˣ
College of Pharmacy
University of Kentucky
Lexington, KY 40506

Received October 9, 1979.
Accepted for publication February 21, 1980.
Supported by FDA Contract 223-77-3001.

Prediction of Steady-State Behavior of Metabolite from Dosing of Parent Drug

Keyphrases □ Metabolism—prediction of steady-state metabolite concentration, cinromide and carbamazepine, monkeys □ Steady-state concentration—prediction of metabolite and parent drug concentrations, metabolism, cinromide and carbamazepine, monkeys □ Cinromide—prediction of steady-state metabolite concentration, monkeys □ Carbamazepine—prediction of steady-state metabolite concentration, monkeys

To the Editor:

It has become apparent that the metabolites of many drugs contribute to the observed clinical efficacy and/or toxicity (1). In assessing the contribution of a given metabolite during chronic dosing, the relative steady-state concentrations of the metabolite and the parent drug (as well as the relative potencies) must be determined. This steady-state ratio was shown to be dependent only on the formation and elimination clearances of the metabolite (2, 3):

$$\frac{C^*_m}{C^*_p} = \frac{Cl_f}{Cl_m} = \frac{f_m Cl_p}{Cl_m} \qquad \text{(Eq. 1)}$$

where C^*_m and C^*_p represent the steady-state plasma concentrations of the metabolite and the parent drug, respectively; Cl_f and Cl_m represent the formation clearance and intrinsic clearance (4) of the metabolite, respectively; f_m is the fraction of the parent drug metabolized to this metabolite; and Cl_p is the systemic clearance of the parent drug.

From Eq. 1, it appears that knowledge of the metabolite clearance and the fraction metabolized (or formation clearance) is necessary to calculate this ratio. The purpose of the present report is to show that the steady-state metabolite to parent drug ratio, as well as the actual steady-state metabolite concentration, can be determined from administration of a single dose of the parent drug without administration of the metabolite. A change in the admin-

0022-3549/80/0500-0610$01.00/0

istration route from systemic to oral results in a first-pass effect for drugs with medium or high extraction ratios. Methods for such corrections are provided. Preliminary experimental data with two drugs support the proposed theoretical approaches.

Equation 1 was derived assuming one-compartmental distribution and first-order elimination for the parent drug and the metabolite. It also is valid if either species (or both) exhibits multicompartmental behavior (mamillary model), as long as elimination occurs from the central compartment.

In Eq. 1, Cl_p and f_m can be expressed in a model-independent manner using areas under the curve (5):

$$Cl_p = \frac{D_p}{(AUC_p)_p} \qquad \text{(Eq. 2)}$$

$$f_m = \left(\frac{(AUC_m)_p}{D_p}\right)\left(\frac{D_m}{(AUC_m)_m}\right) = \left(\frac{(AUC_m)_p}{D_p}\right)Cl_m \qquad \text{(Eq. 3)}$$

where AUC is the area under the plasma concentration (molar)–time curve from zero to infinity; $(AUC_c)_b$ represents the AUC of c after a single dose of b; the subscripts m and p refer to the metabolite and the parent drug, respectively; and D refers to the dose in molar units.

The formation clearance, Cl_f, then is given by the product of Eqs. 2 and 3:

$$Cl_f = \left(\frac{(AUC_m)_p}{(AUC_p)_p}\right)Cl_m \qquad \text{(Eq. 4)}$$

Substitution of Eq. 4 into Eq. 1 shows that the steady-state ratio, C^*_m/C^*_p, becomes equal to the ratio of the areas of the metabolite and the parent drug after a single dose:

$$\frac{C^*_m}{C^*_p} = \frac{(AUC_m)_p}{(AUC_p)_p} \qquad \text{(Eq. 5)}$$

Equation 5 shows that the ratio of the steady-state concentrations of the metabolite and the parent drug can be predicted from concentration–time data obtained after a single intravenous dose of the parent drug. This relationship assumes linearity (with respect to dose and time) for the parent drug and the metabolite. This prediction requires the monitoring of metabolite and parent drug levels but does not require administration of the metabolite.

Equation 5 also can be used to calculate the actual steady-state concentration of the metabolite achieved by a given infusion rate, R_0, of the parent drug:

$$C^*_m = \left(\frac{(AUC_m)_p}{(AUC_p)_p}\right)C^*_p \qquad \text{(Eq. 6)}$$

With Eq. 2, C^*_p can be expressed as:

$$C^*_p = \frac{R_0}{Cl_p} = \frac{R_0(AUC_p)_p}{D_p} \qquad \text{(Eq. 7)}$$

Substitution of C^*_p from Eq. 7 into Eq. 6 yields:

$$C^*_m = \frac{R_0}{D_p}(AUC_m)_p \qquad \text{(Eq. 8)}$$

From a practical point of view, Eq. 8 implies that the steady-state metabolite concentration can be calculated by monitoring only metabolite levels without knowledge of parent drug levels (following administration of a single dose of the parent drug).

Equations 5 and 8 are directly applicable to the multiple dosing situation without any modifications as long as the multiple doses are given by the same route as the single dose (*i.e.*, the same dosage form). When there is a change in the administration route, Eqs. 5 and 8 must be modified. For instance, to estimate the C^*_m/C^*_p ratio after multiple oral doses from areas under the curve obtained after a single intravenous dose, a correction for any first-pass effect of the parent drug must be included so that Eq. 5 becomes:

$$\frac{\overline{C}^*_m}{\overline{C}^*_p} = \left[\frac{(AUC_m)_p}{(AUC_p)_p}\right]_{iv}\frac{1}{F_p} \qquad \text{(Eq. 9)}$$

where F_p represents the fraction of the dose of the parent drug systemically available, and $\overline{C}^*_m$ and $\overline{C}^*_p$ refer to the average concentrations during a dosing interval (a fixed-dose, fixed-time schedule).

Similarly, to estimate the average steady-state concentration of the metabolite after multiple oral doses from the area under the curve obtained after a single intravenous dose, Eq. 8 becomes:

$$\overline{C}^*_m = \left[\frac{(AUC_m)_p}{D_p}\right]_{iv} f_a \times \text{dose rate} \qquad \text{(Eq. 10)}$$

where f_a represents the dose fraction absorbed into the portal circulation; no correction for the first-pass effect of the parent drug is necessary. The applicability of Eqs. 5 and 8 was verified using data obtained during the pharmacokinetic characterization of cinromide and carbamazepine in rhesus monkeys.

Cinromide [(*E*)-*m*-bromo-*N*-ethylcinnamamide], a new antiepileptic drug[1], is metabolized by *N*-deethylation to 3-bromocinnamamide (6, 7). Short-term (not to steady state) and long-term (to steady state) infusions of the parent drug were administered to two monkeys. The C^*_m/C^*_p ratios and C^*_m values for the long-term infusions were predicted from the short infusion studies. Table I shows the agreement between the predicted and experimental values.

Carbamazepine is metabolized to a 10,11-epoxide, and the kinetics of the parent drug and the metabolite were elucidated (2). Single-dose intravenous studies with the parent drug in two monkeys enabled a prediction of C^*_m/C^*_p and C^*_m. These values compared favorably with the corresponding values obtained during a zero-order intravenous infusion of carbamazepine to the steady state (Table I).

The proposed theoretical approach has applications in drug development and in therapeutics. In the preclinical evaluation of new drugs, prediction of steady-state metabolite concentrations is useful in planning efficacy and toxicity studies. Furthermore, clinical monitoring of me-

Table I—Comparison of Predicted and Observed Metabolite to Parent Drug Ratio (C^*_m/C^*_p) and Metabolite Concentration (C^*_m) at Steady State

Monkey	C^*_m/C^*_p Predicted	C^*_m/C^*_p Observed	C^*_m, μg/ml Predicted	C^*_m, μg/ml Observed
	Cinromide and 3-Bromocinnamamide			
184	4.1 ± 0.55[a]	4.5	14.5 ± 2.0	12.3
336	2.9 ± 0.6	3.5	10.6 ± 1.8	10.6
	Carbamazepine and Carbamazepine-10,11-epoxide			
346	0.12	0.15	0.26	0.30
336	0.08	0.08	0.15	0.19

[a] Mean and standard deviation of prediction.

[1] Developed by Burroughs-Wellcome Laboratories, Research Triangle Park, N.C.

tabolites is becoming necessary with several pharmacological classes of drugs (antidepressants, antiarrhythmics, antiepileptics, and steroids).

(1) D. E. Drayer, *Clin. Pharmacokinet.*, 1, 426 (1976).
(2) I. H. Patel, R. H. Levy, and W. F. Trager, *J. Pharmacol. Exp. Ther.*, **206**, 607 (1978).
(3) A. A. Lai, B. H. Min, W. A. Garland, and R. H. Levy, *J. Pharm. Biopharm.*, 7, 87 (1979).
(4) K. S. Pang and J. R. Gillette, *J. Pharmacokinet. Biopharm.*, 7, 275 (1979).
(5) S. A. Kaplan, M. L. Jack, S. Cotler, and K. Alexander, *ibid.*, 1, 201 (1973).
(6) J. S. Lockard, R. H. Levy, L. L. Ducharme, and W. C. Congdon, *Epilepsia*, **20**, 339 (1979).
(7) E. A. Lane and R. H. Levy, "Epilepsy: Vancouver International Symposium," Raven, New York, N.Y., in press.

E. A. Lane
R. H. Levy ˣ
Departments of Pharmaceutical Sciences and Neurological Surgery
Schools of Pharmacy and Medicine
University of Washington
Seattle, WA 98195

Received January 7, 1980.
Accepted for publication February 22, 1980.
Supported by National Institutes of Health Research Contract NO1-NS-1-2282.

Glass Transition Temperature of Citric Acid

Keyphrases □ Glass transition temperature—citric acid, glass formation, temperature variations due to water loss variations □ Citric acid—glass formation, glass transition temperature, comparison of anhydrous and monohydrate forms of citric acid □ Glass formation—citric acid, glass transition temperature

To the Editor:

A recent publication (1) examined solid dispersion systems using techniques similar to those we described previously (2, 3). Discrepancies between the glass transition temperature observed by the two groups of investigators (33–36°) have been explained as being due to an artifact. We hope the present observations will clarify the matter.

The glass transition temperature cannot be given an absolute value other than that extrapolated to a zero heating rate (4), because it is dependent on the rate of quenching of the glass and the heating rate employed to measure the transition. This was shown clearly by Rötger (5), who characterized the glass transition temperature by two rate indexes applicable to the quenching and heating rates of the sample. One immediate difference between the two reported studies (1, 3) was the heating rate employed during the measurement of the glass transition. Timko and Lordi (1) used 10°/min, whereas we used 2°/min (3). We also quoted the glass transition temperature as the onset of the transition (first deviation from the thermogram[1] baseline) rather than the extrapolated onset of Timko and Lordi (1), because this approach appeared to give better precision with different sample sizes. At 2°/min, the difference between the extrapolated onset and the initial deviation is only ~0.5–1°.

[1] D.S.B.1B, Perkin-Elmer, Beaconsfield, England.

Table I—Effect of Water on Glass Transition Temperature

Water Added to Melt, % (w/w)	Glass Transition Temperature
3	−8–−13°
4	−13–−18°
5	−23–−26°

However, these two differences do not account for the large discrepancy reported in the two studies. For example, with our methods, the glass transition temperature of anhydrous citric acid was 7°, rather than 10° as quoted by Timko and Lordi (1).

The second difference in the two studies was the use of citric acid monohydrate (2, 3) rather than anhydrous citric acid. We believe that the discrepancy in the glass transition temperature of the two materials is due to the water bound in the glass of the monohydrate, which is difficult to remove from the melt at 150° (the temperature used in our method). This concept is in agreement with our previous suggestion (2) that using the monohydrate is advantageous because of the formation of a citric acid solution.

Since the devitrified glasses contain anhydrous citric acid, water probably is lost during crystallization of the melt and should be detectable as a weight loss. We measured the weight loss on devitrification and drying at 60° after heating the monohydrate melt for varying periods at 140–150°. After 4 min of heating, the weight loss was 4.8–5.6% (w/w); after 10 min of heating, it was reduced only to 4.3–5.3% (w/w).

The effect of water on the glass transition temperature can be shown by incorporating water into a melt of anhydrous citric acid produced by the method outlined previously (2) and above and measuring the glass transition temperature as described previously (3). The results are shown in Table I. There is some variation in the glass transition temperature due to variation in water loss on its addition to the melt. However, if the water is added when the melt is relatively cool, it induces crystallization; therefore, the system has to be reheated, resulting again in loss of water. These results are consistent with the reported weight losses and suggest that ~4.5% moisture is in the glass. If 9% (w/w) water (the amount present in the monohydrate) is added to anhydrous citric acid before melting and the glass preparation method is repeated, the glass transition temperature is −23–−24°, which is consistent with our previous results.

The results suggest that when the monohydrate is used, an unavoidable amount of water is present in the glass, which affects the glass transition temperature. This effect is reproducible, suggesting a consistent amount of entrapment in the melt. Furthermore, the properties of the anhydrous and monohydrate glasses are similar because, as a continuation of previous work (6), we found that the effect of phenobarbital on the citric acid (monohydrate) transition temperature was similar to that reported by Timko and Lordi (1).

(1) R. J. Timko and N. G. Lordi, *J. Pharm. Sci.*, **68**, 601 (1979).
(2) M. P. Summers and R. P. Enever, *ibid.*, **65**, 1613 (1976).
(3) *Ibid.*, **66**, 825 (1977).
(4) J. P. Mercier and J. J. Aklonis, *J. Paint Technol.*, **43**, 44 (1974).
(5) H. Rötger, in "Amorphous Materials," R. W. Douglas and B. Ellis, Eds., Wiley-Interscience, London, England, 1972.

0022-3549/80/0500-0612$01.00/0